An improved nonlinear model of HEMTs with independent transconductance tail-off fitting

Liu Linsheng(刘林盛)†

School of Electronic Engineering, University of Electronic Science and Technology of China, Chengdu 611731, China

Abstract: We present an improved large-signal device model of GaAs/GaN HEMTs, amenable for use in commercial nonlinear simulators. The proposed model includes a new exponential function to independently control the transconductance compression/tail-off behaviors. The main advantage of this model is to provide a simple and coherent description of the bias-dependent drain current (I–V) that is valid in all regions of operation. All aspects of the model are validated for 0.25-μm gate-length GaAs and GaN HEMT processes. The simulation results of DC/pulsed I–V, RF large-signal power and intermodulation distortion products show excellent agreement with the measured data.

Key words: large-signal model; parameter extraction; HEMT

DOI: 10.1088/1674-4926/32/2/024004 **PACC:** 7340Q; 1110L

1. Introduction

The availability of general-purpose Harmonic-Balance and Volterra-Series simulators has generated a need for accurate nonlinear models of various devices, such as HEMTs, MESFETs and LDMOSFETs[1]. In the computer-aided design (CAD) and analysis of microwave circuits, the device model is required to predict the output power, power-added-efficiency (PAE), higher-order harmonics, IMD performances, etc.

One of the major nonlinearities in III–V field effect transistors (FETs) is from bias-dependent drain-current I–V relationships[2]. In addition, due to the complexity in heterostructures of HEMTs and the associated physical characteristics, they are most appropriately modeled based on semi-empirical approach with parameters extracted from measurements[1−7]. Among them, the widely-used Angelov HEMT I–V model[3] is one of the most successful models by virtue of its simplicity, higher-order differentiability, good convergence performance and well-defined fitting parameters[8]. However, the Angelov model sometimes faces accuracy issues, where compromises have to be made for the overall fitting[4−7].

For this purpose, we present an improved large-signal I–V model of HEMTs with the Angelov model as prototype. By maintaining the merits of the original one, the proposed model is capable of representing the nonlinear I–V relationships between and across the entire bias range of different regimes. This has been done by introducing a new exponential function to independently control the transconductance ($G_{\rm m}$) tail-off characteristics found in most HEMTs. Excellent agreement is observed between measured and simulated results by utilizing a 0.25-μm gate-length GaAs double-heterojunction δ-doped pHEMT and a GaN metal–insulator–semiconductor HEMT (MISHEMT)[9] with an atomic-layer-deposited (ALD) Al_2O_3 gate insulator on a high-resistivity silicon (111) substrate ($>$ 10000 $\Omega\cdot$ cm).

2. Model description

2.1. Review of the Angelov I–V model

The equation-based nonlinear Angelov HEMT I–V/$G_{\rm m}$–V model is in the form of the following expressions[2],

$$I_{\rm ds}(V_{\rm gs}, V_{\rm ds}) = I_{\rm ds1}(V_{\rm gs}, V_{\rm ds})I_{\rm ds2}(V_{\rm gs}, V_{\rm ds}), \tag{1}$$

where

$$I_{\rm ds1}(V_{\rm gs}, V_{\rm ds}) = I_{\rm pk}(1 + \tanh\psi), \tag{2}$$

$$\psi = P_1V_{\rm gsp} + P_2V_{\rm gsp}^2 + P_3V_{\rm gsp}^3 + \cdots, \tag{3}$$

$$V_{\rm gsp} = V_{\rm gs} - V_{\rm pko} - w_0V_{\rm ds}, \tag{4}$$

$$I_{\rm ds2}(V_{\rm gs}, V_{\rm ds}) = \tanh(\alpha V_{\rm ds})(1 + \lambda V_{\rm ds}), \tag{5}$$

$$G_{\rm m} = \partial I_{\rm ds}/\partial V_{\rm gs} = I_{\rm pk}\sec h^2(\psi) \times \partial\psi/\partial V_{\rm gs} \times I_{\rm ds2}. \tag{6}$$

The second part $I_{\rm ds2}$ in Eq. (1) is to model the drain-voltage ($V_{\rm ds}$) dependent characteristics. This part keeps very similar formulation for different empirical I–V models, aimed at describing the knee voltage due to the on-resistance and the non-zero drain conductance in saturation regions. $I_{\rm ds1}$ is used to primarily describe the $I_{\rm ds}$–$V_{\rm gs}$ ($G_{\rm m}$–$V_{\rm gs}$) relation, and the main differences in the existing equation-based empirical I–V models are the forms of this function[10].

In the Angelov model, the key model parameters in the $I_{\rm ds1}$ equation (2), such as the peak $G_{\rm m}$ coefficient (P_1), gate voltage ($V_{\rm pk}$) and drain current ($I_{\rm pk}$) for maximum $G_{\rm m}$, etc, determine the I–V/$G_{\rm m}$–V shapes and the modeling performances in the entire bias range. Those parameters can be extracted directly from the measured peak $G_{\rm m}$ points[8]. Subsequently, the $G_{\rm m}$ curves can be partitioned into two portions: $G_{\rm m}$ expansion from the pinch-off to turn on when $V_{\rm gs} < V_{\rm pk}$ and $G_{\rm m}$ compression from maximum to tail-off when $V_{\rm gs} > V_{\rm pk}$. Then the left fitting parameters in the power series function ψ (usually P_2 and P_3) are used to refine the $G_{\rm m}$–$V_{\rm gs}$ curves for both parts[6].

† Corresponding author. Email: llsheng617@gmail.com
Received 10 August 2010, revised manuscript received 14 October 2010

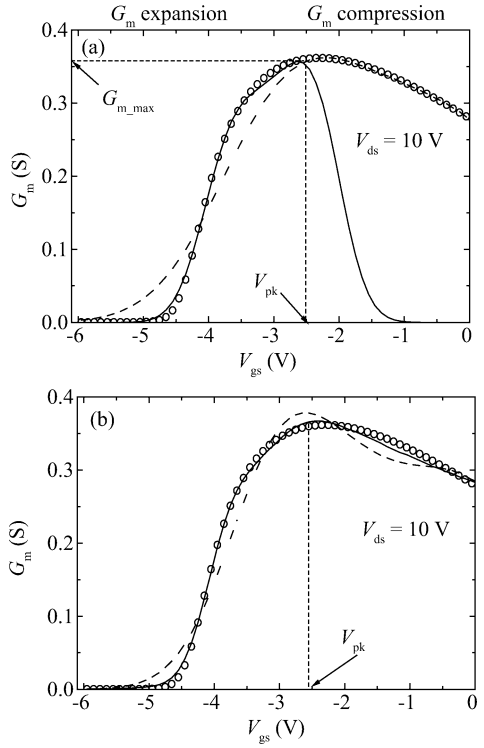

Fig. 1. (a) Angelov I–V model optimized for the G_m expansion part (solid lines) and the G_m compression part (dashed lines) fitted to the measured data (symbols) of a GaN HEMT on a Si substrate[7]. (b) Angelov I–V model optimized for the overall fitting (dashed lines) and the improved I–V model (solid lines) fitted to the measured data (symbols).

2.2. Restriction in the Angelov model

To extract the model parameters in the Angelov I–V model, there is one restriction to be satisfied[3]: the saturation current I_{sat} is about twice that of I_{pk}. It is reported in Refs. [5, 11] that this condition is too stringent to be satisfied by the measurements, where the Angelov model cannot reproduce the measured I–V/G_m–V characteristics as well as the higher-order derivatives, even higher-order terms of the polynomial expansion in Eq. (3) have been used.

To graphically interpret the operation of the Angelov model, the measured data of a GaN HEMT on Si in Ref. [5] has been reconstructed. It can be seen in Fig. 1(a) that the Angelov model can actually perform quite well for either the G_m expansion or the G_m compression part. And similar capability of the Angelov model to fit half of the G_m–V curve has also been demonstrated in Ref. [12] for SiC MESFET modeling without a G_m compression mechanism. However, for the overall fitting of the GaN HEMT with typical bell-shaped G_m characteristics, the accuracy of the Angelov model will become limited and compromises have to be made[5], as compared in Fig. 1(b).

2.3. The improved large-signal model

To solve this problem, a modified analytical drain-current I–V model is proposed, as follows,

$$I_{ds}(V_{gs}, V_{ds}) = I_{angelov} + I_{Gmtail}, \tag{7}$$

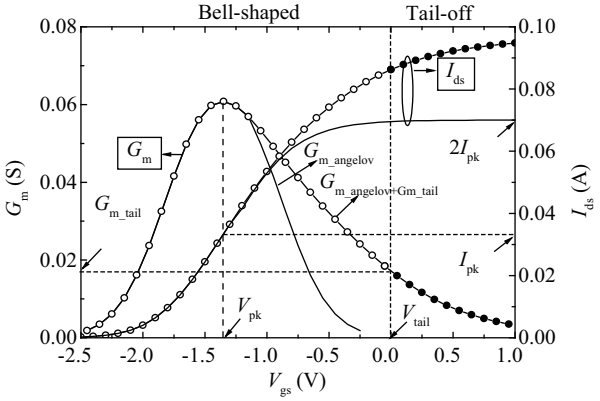

Fig. 2. Graphical interpretations of the proposed nonlinear I–V model.

$$I_{angelov} = I_{pk}(1 + \tanh(ph))\tanh(\alpha_1 V_{ds}), \tag{8}$$

$$I_{Gmtail} = G_{mtail} V_{efft} \tanh(\alpha_2 V_{ds}), \tag{9}$$

$$ph = P_1 V_{gsp} + P_2 V_{gsp}^2 + P_3 V_{gsp}^3 + ..., V_{gsp} = V_{eff11} - V_{pk}, \tag{10}$$

$$\begin{cases} V_{efft} = \dfrac{1}{m_1}\dfrac{1}{m_2}[1 - (1 + m_2 V_{eff12})^{-m_1}], & m_1 > 0, \\ V_{efft} = \dfrac{1}{m_2}\ln(1 + m_2 V_{eff12}), & m_1 = 0, \end{cases} \tag{11}$$

$$V_{eff11} = (V_{gst} - V_{gsta})/2 + V_{tail}, V_{eff12} = (V_{gst} + V_{gsta})/2, \tag{12}$$

$$V_{gst} = V_{gs} - V_{tail}, V_{gsta} = \frac{1}{n}\ln(2\cosh(nV_{gst})), \tag{13}$$

$$V_{pk} = V_{pko} + w_0 V_{ds}, V_{tail} = V_{tailo} + w_1 V_{ds}. \tag{14}$$

As described in Fig. 2, the developed HEMT I–V model (7) consists of two parts. $I_{angelov}$ maintains the characteristics of the Angelov model, where the extraction of the key model parameters (P_1, V_{pk} and I_{pk}) at maximum G_m is still the same as in the original model. In addition, the tuning parameters in the ph function (P_2 and P_3) now have more freedom to model the G_m expansion when $V_{gs} < V_{pk}$ for the threshold region and the transition from pinch-off to turn-on. The added I_{tail} part (3) is to independently model the G_m compression behaviors distinguished by the V_{tail} parameter, the turning point of gate voltage where G_m tail-off begins.

This modification with a multiplier term allows the elongation of the bell-shape G_m for $V_{gs} > V_{pk}$. Since the restriction of the "symmetrical" behavior of $2I_{pk} = I_{sat}$ in the original Angelov model confines its range of operation[10, 11], the inclusion of the I_{tail} current source permits the drain current to increase beyond $2I_{pk}$ as a function of V_{gs} and results in significantly improved accuracy. As a consequence, no trade-offs need to be made for the overall fitting, and the improved I–V model enhances its bias range of operation for which accuracy is maintained.

Moreover, in order to characterize the charge-trapping and self-heating effects[13] found in most GaAs/GaN HEMTs[7], a four-terminal large-signal equivalent-circuit topology with frequency dispersion and thermal sub-circuits has been employed[14], as shown in Fig. 3. The trapping and temperature coefficients as the correction of the model parameters in Eq. (15) are then determined by comparing the pulsed I–V

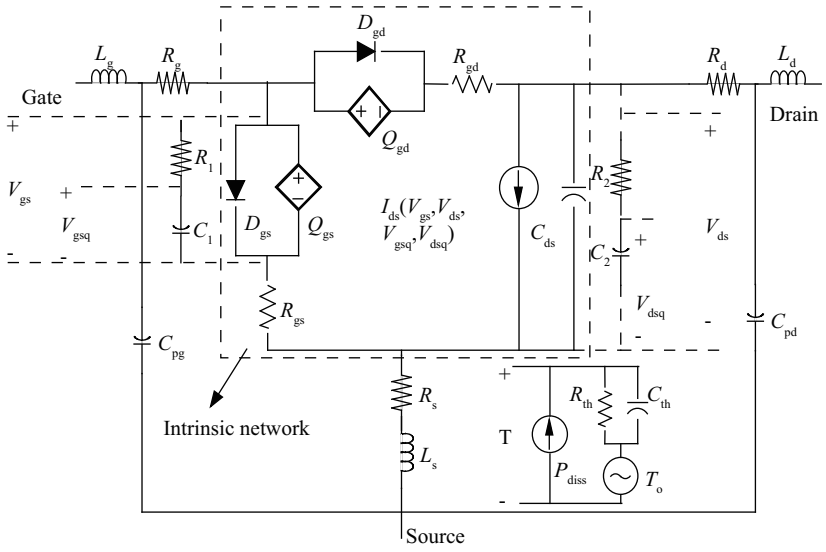

Fig. 3. Complete "four-terminal" large-signal equivalent circuit of HEMTs.

characteristics at different quiescent biasing points and ambient temperatures[10, 12],

$$I_{ds} = I_{ds}(V_{gs}, V_{ds}, V_{gsq}, V_{dsq}),$$

where

$$\begin{aligned}
P_1 &= \frac{P_{1o}}{((1 + P_{1vdsq}\Delta V_{dsq})(1 + P_{1vgsq}\Delta V_{gsq}))} + P_{1t}\Delta T,\\
I_{pk} &= I_{pk0} + I_{pkvdsq}\Delta V_{dsq} + I_{pkvgsq}\Delta V_{gsq} + I_{pkt}\Delta T,\\
G_{mtail} &= G_{mtailo} + G_{mtailvdsq}\Delta V_{dsq} + G_{mtailvgsq}\Delta V_{gsq}\\
&\quad + G_{mtailt}\Delta T,\\
V_{pk} &= V_{pko} + V_{pkvdsq}\Delta V_{dsq} + V_{pkvgsq}\Delta V_{gsq} + w_1 V_{ds},\\
V_{tail} &= V_{tailo} + V_{tailvdsq}\Delta V_{dsq} + V_{tailvgsq}\Delta V_{gsq} + w_2 V_{ds},\\
\alpha_1 &= \frac{\alpha_{1o}}{(1 + \alpha_{1vdsq}\Delta V_{dsq})},\ \alpha_2 = \frac{\alpha_{2o}}{(1 + \alpha_{2vdsq}\Delta V_{dsq})},\\
\Delta V_{dsq} &= V_{dsq} - V_{dso},\ \Delta V_{gsq} = V_{gsq} - V_{gso},\\
\Delta T &= \Delta T_o + R_{th}\Delta P_{diss}.
\end{aligned} \tag{15}$$

In addition, in the equivalent-circuit large-signal model shown in Fig. 3, the extrinsic elements were first determined from multi-bias S-parameter measurements using standard cold-FET methods[15]. Then the extracted multi-bias C_{gs} and C_{gd} were fitted using the charge-conservative gate charge model[16]. Finally, the nonlinear gate–source and gate–drain diodes were modeled using the Shockley ideal diode equation. And the complete nonlinear model was implemented as a user-defined model (SDD) in Agilent's ADS.

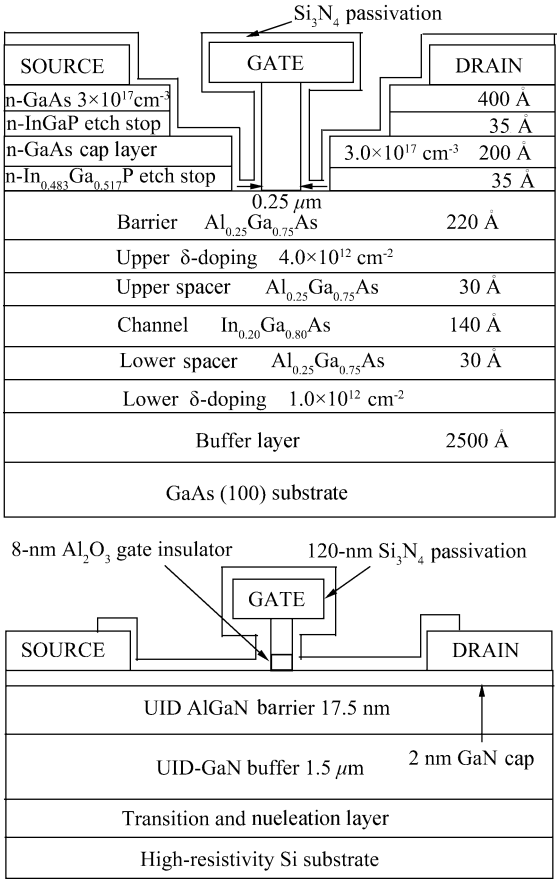

Fig. 4. Physical layer structure of the modeled (a) GaAs pHEMT and (b) GaN MISHEMT.

3. Experimental model verification

In order to demonstrate the usefulness of the proposed large-signal model, the 0.25-μm gate-length on-wafer GaAs double-heterojunction δ-doped pHEMT[7] and the high-power density GaN metal–insulator–semiconductor HEMT (MISHEMT) with atomic-layer-deposited (ALD) Al_2O_3 gate insulator[9] have been modeled and validated. The physical layer structures of the experimented GaAs and GaN HEMTs are shown in Figs. 4 (a) and 4(b), respectively.

As a first step, isothermal pulsed I–V measurements[17] for the 2 ×100 μm gate-width GaAs and GaN HEMTs have been investigated for verification of the drain-current model. The extracted model characteristics at the quiescent biasing point of (V_{gsq}, V_{dsq}) = (0 V, 0 V) are compared to measured

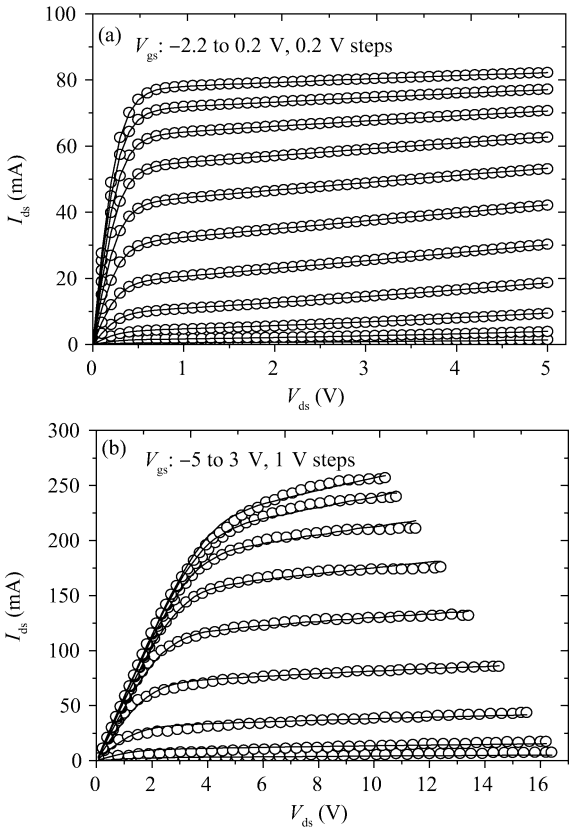

Fig. 5. Measured (circles) and modeled (solid lines) pulsed I–V characteristics at (V_{gsq}, V_{dsq}) = (0 V, 0 V). (a) GaAs pHEMT. (b) GaN MISHEMT.

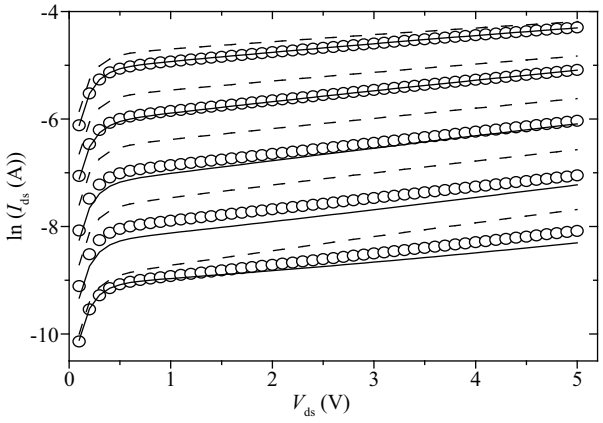

Fig. 6. The improved model (solid lines), Angelov model (dashed lines), and measurements (symbols) of the GaAs pHEMT pulsed I–V characteristics by highlighting the pinch-off levels, V_{gs} = –2.2 V to –1.4 V, 0.2 V steps.

values in Figs. 5 (a) and 5(b), where an excellent fit is obtained for the entire bias range. In addition, Figure 6 highlights the excellent agreement at pinch-off levels of the GaAs pHEMT using a logarithmic scale. The fitting parameters of the improved model and the Angelov model are listed in Table 1. The results in Figs. 7(a) and 7(b) demonstrate that there is good agreement between the model output and measurements under different quiescent biasing points of the DC/pulsed I–V characteristics.

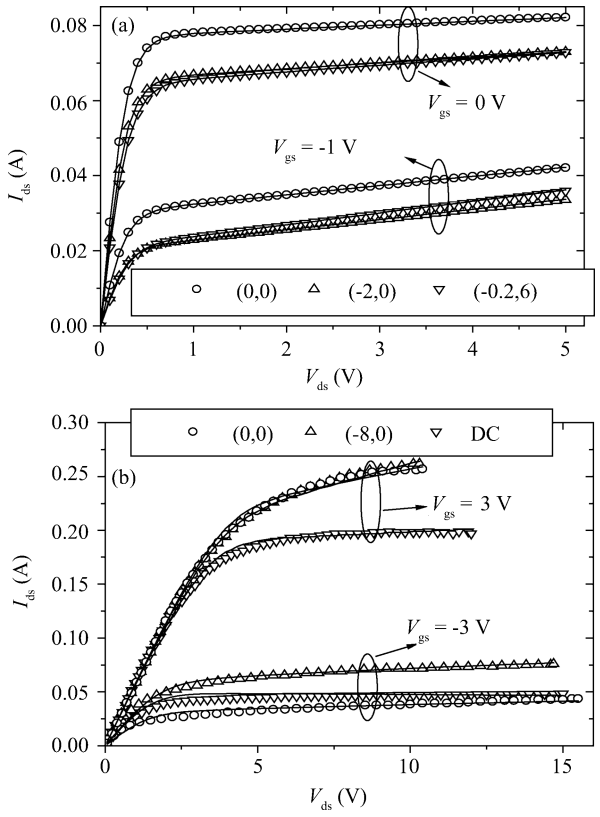

Fig. 7. Measured (symbols) and modeled (lines) pulsed I–V characteristics under different quiescent biasing conditions. (a) GaAs pHEMT. (b) GaN MISHEMT.

The performance of the model is also validated by comparing the higher-order derivative products of the drain current. The modeled and measured first three derivatives (G_m, G_{m2} and G_{m3}) of the two HEMT devices with respect to gate voltage are shown in Figs. 8 (a) and (b). These curves serve to illustrate the improvements in the derivative reproduction of the modified I–V model over the original one.

The utility of the model power performance is verified by comparing its output predictions with measured power data. The transmitted output power characteristics for the first three harmonics, power gain, and power-added-efficiency (PAE) at a particular biasing point in deep Class-AB biasing conditions are simulated and compared with measured data, as shown in Figs. 9(a) to 9(d), respectively. The input and output terminating impedances of the device were adjusted for maximum PAE performances. It can be seen that the proposed large-signal model provides a very good prediction of the power characteristics. Moreover, the third-order intermodulation distortion (IMD) has been characterized using two-tone tests under 50 Ω biasing conditions. According to the data and simulated output compared in Fig. 9, the developed nonlinear model is capable of predicting the one-tone harmonic power levels as well as two-tone higher-order IMD products more accurately.

4. Conclusion

An improved large-signal drain-current model has been presented and validated for GaAs/GaN HEMTs. By employing a new exponential function to independently control the G_m

Table 1. Extracted fitting parameters of the improved model and the angelov model.

	Param.	I_{pk} (A)	V_{pko} (V)	P_1 (V^{-1})	P_2 (V^{-2})	P_3 (V^{-3})	α_1 (V^{-1})	w_o	α_2 (V^{-1})	w_1	m_1	m_2 (V^{-1})	G_{mtail} (S)	V_{tailo} (V)	n
GaAs	Angelov	0.046	–0.73	1.23	–0.24	0.20	3.74	–0.040	–	–	–	–	–	–	–
	Improved	0.056	–0.64	1.08	–0.31	0.38	3.74	–0.040	3.80	–0.041	2.09	1.41	0.012	0.14	1.01
GaN	Angelov	0.14	–0.87	0.38	–0.03	0	0.67	–0.022	–	–	–	–	–	–	–
	Improved	0.15	–0.84	0.36	–0.04	0.006	0.67	–0.022	0.70	–0.023	0.81	1.67	0.021	2.31	0.40

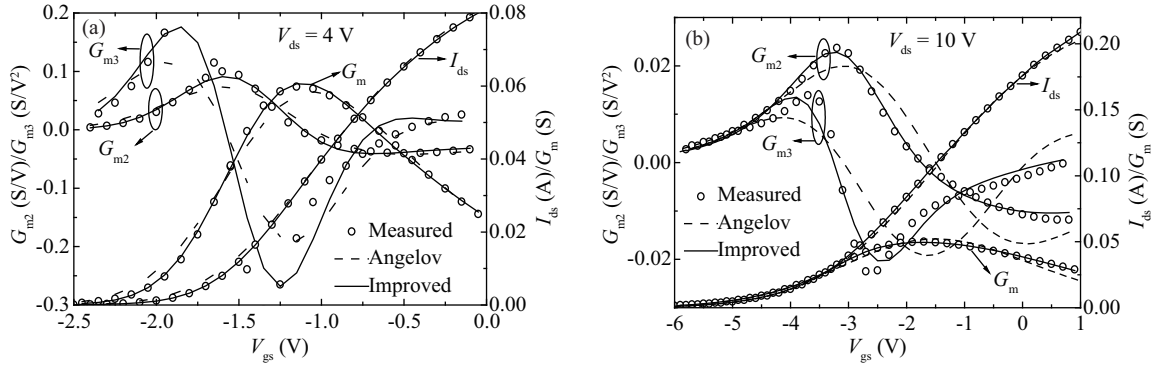

Fig. 8. Measured (circles) and modeled (lines) pulsed I–V and its first three derivatives (G_m, G_{m2} and G_{m3}) characteristics. (a) GaAs pHEMT. (b) GaN MISHEMT.

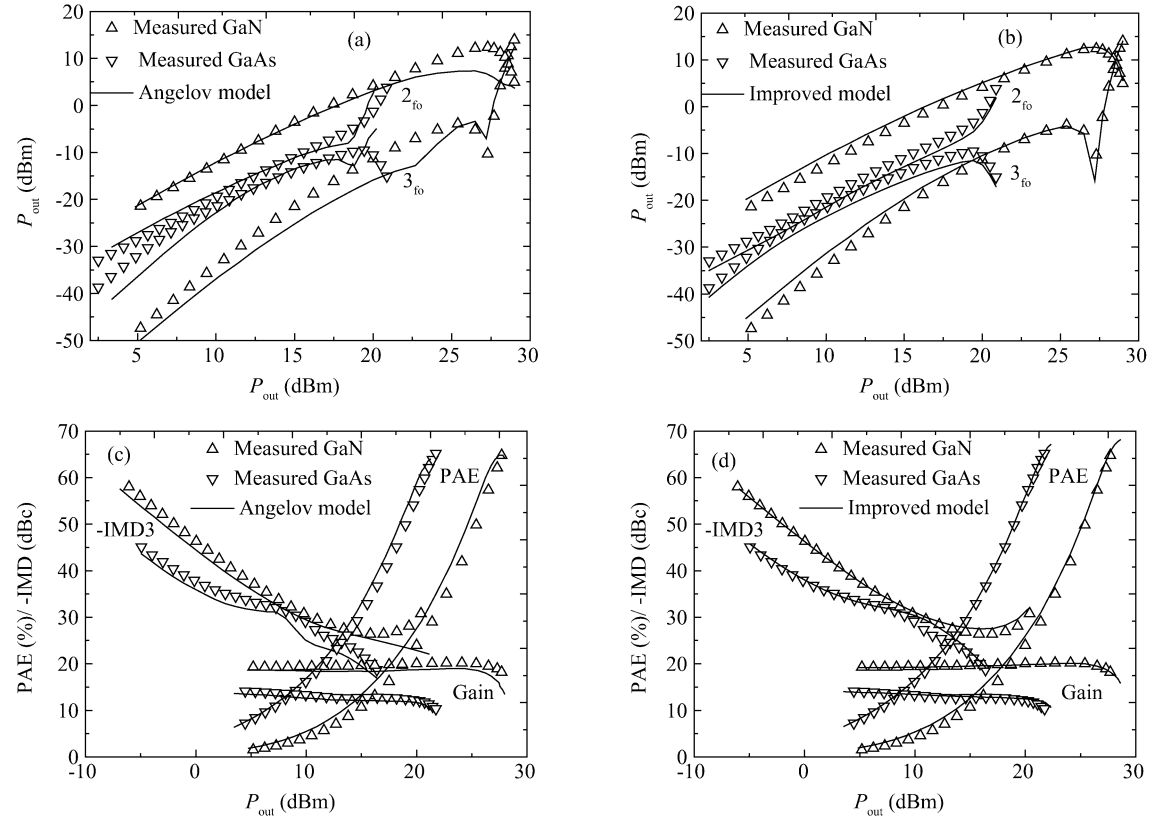

Fig. 9. (a), (b) Measured (symbols) and modeled (lines) results for the output harmonic power levels at fundamental frequency of GaAs: 7.5 GHz biased at (–1.8 V, 6 V), and GaN: 4 GHz biased at (–3.8 V, 20 V). (c), (d) Measured (symbols) and modeled (lines) single-tone PAE and two-tone (tone spacing of 10 MHz) third-order IMD performances.

tail-off region where the drain current is approaching saturation, the modeling accuracy will be increased especially for the drain current at gate voltage close to pinch-off or under open channel, which is often compromised in the original Angelov model. The modified nonlinear I–V model has demonstrated the ability to model the dynamic pulsed I–V characteristics of the GaAs and GaN HEMTs under various quiescent biases. In addition, the complete large-signal model has been implemented in Agilent's ADS and can accurately predict the large-signal output power performances for first three harmonics as

well as two-tone IMD characteristics. The proposed model developed from the widely-used Angelov HEMT $I-V$ model is also kept easy to extract, so it can serve as a useful tool in commercial nonlinear simulators.

References

[1] Gao J J. RF and microwave modeling and measurement techniques for compound field effect transistors. Raleigh: SciTech Publishing, 2009

[2] Angelov I, Zirath H, Rorsman N. A new empirical model for HEMT and MESFET devices. IEEE Trans Microwave Theory Tech 1992, 40: 2258

[3] Angelov I, Bengtsson L, Garica M. Extensions of the Chalmers nonlinear HEMT and MESFET model. IEEE Trans Microwave Theory Tech, 1996, 44: 1664

[4] Ooi B L, Ma J Y, Leong M S. A new MESFET nonlinear model. Microwave Opt Technol Lett, 2001, 29: 226

[5] Cabral P, Pedro J, Carvalho N. New nonlinear device model for microwave power GaN HEMTs. IEEE MTT-S Int Microwave Symp Dig, 2004: 51

[6] Liu L S, Ma J G. Improved drain–source current model for HEMT's with accurate G_{m} fitting in all regions. IEEE Compound Semiconductor IC Symp Dig, 2008: 1

[7] Liu L S, Ma J G, Ng G I. Electrothermal large-signal model of III–V FETs accounting for frequency dispersion and charge conservation. IEEE MTT-S Int Microwave Symp Dig, 2009: 749

[8] Loo-Yau J R, Reynoso-Hernández J A, Auñiga J E, et al. Modeling the $I-V$ characteristics of the power microwave FETs with the Angelov model using pulse measurements. Microwave Opt Technol Lett, 2006, 48: 1046

[9] Liu Z H, Ng G I, Arulkumaran S, et al. High microwave-noise performance of AlGaN/GAN MISHEMTs on silicon with Al_2O_3 gate insulator grown by ALD. IEEE Electron Device Lett, 2010, 31: 96

[10] Liu L S, Ma J G, Ng G I. Electrothermal large-signal model of III–V FETs including frequency dispersion and charge conservation. IEEE Trans Microwave Theory Tech, 2009, 57: 3106

[11] Yuk K S, Branner G R, McQuate D J. A wideband multiharmonic empirical large-signal model for high-power GaN HEMTs with self-heating and charge-trapping effects. IEEE Trans Microwave Theory Tech, 2009, 57: 3322

[12] Yuk K S, Branner G R. An empirical large-signal model for SiC MESFETs with self-heating thermal model. IEEE Trans Microwave Theory Tech, 2008, 56: 2671

[13] Deng J, Wang W, Halder S, et al. Temperature-dependent RF large-signal model of GaN-based MOSHFETs. IEEE Trans Microwave Theory Tech, 2008, 56: 2709

[14] Brady R G, Rafael-Valdivia G, Brazil T. Large-signal FET modeling based on pulsed measurements. IEEE MTT-S Int Microwave Symp Dig, 2007: 593

[15] Dambrine G, Cappy A, Heliodore F, et al. A new method for determining the FET small-signal equivalent circuit. IEEE Trans Microwave Theory Tech, 1988, 36: 1154

[16] Liu L S, Ma J G, Ng G I, et al. Nonlinear HEMT model direct formulated from the second-order derivative of the $I-V/Q-V$ characteristics. IEEE MTT-S Int Microwave Symp Dig, 2010: 1676

[17] DIVA user manual. Accent Opt Technol Inc., Bend, OR, 2001